Cyclin A Is Destroyed in Prometaphase and Can Delay Chromosome Alignment and Anaphase✪

Nicole den Elzen and Jonathon Pines

Wellcome/Cancer Research Campaign Institute, Cambridge CB2 1QR, United Kingdom

Abstract. Mitosis is controlled by the specific and timely degradation of key regulatory proteins, notably the mitotic cyclins that bind and activate the cyclin-dependent kinases (Cdks). In animal cells, cyclin A is always degraded before cyclin B, but the exact timing and the mechanism underlying this are not known. Here we use live cell imaging to show that cyclin A begins to be degraded just after nuclear envelope breakdown. This degradation requires the 26S proteasome, but is not affected by the spindle checkpoint. Neither deletion of its destruction box nor disrupting Cdk binding prevents cyclin A proteolysis, but Cdk binding is necessary for degradation at the correct time. We also show that increasing the levels of cyclin A delays chromosome alignment and sister chromatid segregation. This delay depends on the proteolysis of cyclin A and is not caused by a lag in the bipolar attachment of chromosomes to the mitotic spindle, nor is it mediated via the spindle checkpoint. Thus, proteolysis that is not under the control of the spindle checkpoint is required for chromosome alignment and anaphase.

Key words: cyclin • proteolysis • chromosome • mitosis • cell cycle

Introduction

In animal cells, the mitotic cyclins A and B are required for entry into mitosis. But, equally as important, their removal is essential for exit from mitosis (for review see Norbury and Nurse, 1993). A nondegradable version of cyclin B arrests cells at the end of anaphase (Holloway et al., 1993; Wheatley et al., 1997), but it is unclear how cells respond to nondegradable cyclin A: cleaving *Xenopus* embryos arrest with condensed chromosomes (Luca et al., 1991) and *Drosophila* cells exhibit a delay, rather than a permanent arrest, in metaphase (Sigrist et al., 1995).

The central role of ubiquitin-mediated degradation in the regulation of mitosis is firmly established (for review see King et al., 1996a). Ubiquitin-mediated degradation entails the covalent attachment of ubiquitin to target proteins by an ubiquitin carrier protein (E2) and usually an ubiquitin ligase (E3) (Hershko and Ciechanover, 1998). In mitosis, the major E3 complex is the anaphase-promoting complex (APC)[1]/cyclosome (King et al., 1995; Sudakin et al., 1995). The APC is under complex control via phosphorylation and by binding one of two WD 40 repeat proteins: Cdc20 and Cdh1/Hct1 in yeast, Fizzy and Fizzy-related in *Drosophila*, or p55cdc/hCdc20 and hCdh1 in humans (for review see Morgan, 1999). In early mitosis the APC binds Cdc20 and recognizes proteins containing a 9–amino acid RxxLxxxxN motif called the "destruction box" (D-box) (Glotzer et al., 1991; Yamano et al., 1998). This motif is required for the degradation of both cyclin B1 and the anaphase inhibitor, securin, in metaphase (for review see Yamano et al., 1998).

The APC is regulated by the spindle checkpoint, which delays anaphase should any chromosome not attach to both poles of the spindle (Rieder et al., 1994, 1995; Li and Nicklas, 1995). The checkpoint acts via a signal transduction pathway composed of the Mad and Bub proteins to inactivate Cdc20 (Hardwick, 1998; for review see Taylor, 1999). This prevents the degradation of securin and consequent chromosome segregation until all the chromosomes are attached to both spindle poles (Yamamoto et al., 1996; Alexandru et al., 1999).

Both cyclins A and B1 are degraded in mitosis by ubiquitin-mediated proteolysis (Glotzer et al., 1991; Hershko et al., 1994; King et al., 1995; Sudakin et al., 1995) and their degradation pathways share common components. The APC can ubiquitylate cyclins A and B1 in vitro (Sudakin et al., 1995) and a dominant negative mutant of the human E2, Ubc10, arrests cells in mitosis with high levels of cyclins A and B1 (Townsley et al., 1997; Bastians et al., 1999). Both cyclin A and B1 have an NH_2-terminal D-box that is required for their degradation in *Xenopus* oocyte extracts (Glotzer et al., 1991; Kobayashi et al., 1992; Lorca et al., 1992a; King et al., 1996b). A functional D-box is also required for the mitotic degradation of human cyclin B1 in vivo (Clute and

✪The online version of this article contains supplemental material.

Address correspondence to Jonathon Pines, Wellcome/Cancer Research Campaign Institute, Tennis Court Road, Cambridge CB2 1QR, UK. Tel.: (44) 1223-334096. Fax: (44) 1223-334089. E-mail: j.pines@welc.cam.ac.uk

[1]*Abbreviations used in this paper:* APC, anaphase-promoting complex; CAK, Cdk–activating kinase; Cdk, cyclin-dependent kinase; CFP, cyan fluorescent protein; D-box, destruction box; DIC, differential interference contrast; GFP, green fluorescent protein; GST, glutathione *S*-transferase; NEBD, nuclear envelope breakdown; YFP, yellow fluorescent protein.

Pines, 1999). The D-box has not been shown directly to be required for the degradation of human cyclin A, but deleting the first 70 amino acids, including the D-box, prevents its degradation in human G1 phase extracts (Bastians et al., 1999). However, substituting the D-box of *Xenopus* cyclin B1 with that of *Xenopus* cyclin A renders cyclin B1 nondegradable in *Xenopus* extracts, whereas the D-box of cyclin B1 supports the proteolysis of cyclin A (King et al., 1996b; Klotzbucher et al., 1996). In addition, the degradation in vitro of *Xenopus* cyclin B1 does not require it to bind its cyclin-dependent kinase (Cdk) partner, but this is required for the degradation of *Xenopus* cyclin A (Stewart et al., 1994).

The differences between cyclin A and B degradation may be relevant to the observation that activating the spindle checkpoint by disrupting the spindle with nocodazole or colchicine inhibits the degradation of cyclin B, but not cyclin A (Pines and Hunter, 1990; Whitfield et al., 1990; Hunt et al., 1992; Bastians et al., 1999). However, in apparent contradiction to this, a mutation in *fizzy*, a downstream target of the spindle checkpoint, prevents the degradation of both *Drosophila* cyclins A and B (Dawson et al., 1995; Sigrist et al., 1995). Similarly, adding anti-Fizzy antibodies to *Xenopus* egg extracts stabilizes both A and B type cyclins (Lorca et al., 1998).

To understand how cyclin A is degraded and how ubiquitin-mediated degradation is regulated during mitosis, the timing of cyclin A degradation must first be determined. In all systems studied thus far cyclin A is always degraded before cyclin B1 (Luca and Ruderman, 1989; Lehner and O'Farrell, 1990; Minshull et al., 1990; Pines and Hunter, 1990, 1991; Whitfield et al., 1990; Hunt et al., 1992). Human cyclin B1 begins to be degraded at the beginning of metaphase (Clute and Pines, 1999), consistent with its inhibition by the spindle checkpoint. However, the precise timing of cyclin A degradation is still unclear. From immunofluorescence studies, it has been reported that human cyclin A protein levels decrease at any time from prometaphase to late anaphase (Pines and Hunter, 1991; Pagano et al., 1992; Girard et al., 1995).

We have used green fluorescent protein (GFP)-linked cyclin A, together with time-lapse fluorescence and differential interference contrast (DIC) microscopy, to analyze the dynamics of cyclin A degradation in mammalian cells in real time. Our results indicate that cyclin A is degraded via a D-box–independent mechanism once the nuclear envelope has broken down (NEBD) and implicate ubiquitin-mediated degradation in chromosome alignment.

Materials and Methods

Cell Culture and Synchronization

HeLa cells and PtK_1 cells were cultured and synchronized as described previously (Clute and Pines, 1999).

Construction of cDNA Plasmids

All cyclin A fusion proteins and mutations were constructed by PCR using Vent polymerase (New England Biolabs, Inc.), cloned into appropriate vectors, and confirmed by automated sequencing. Myc-tagged *Hs* cyclin A–GFP (Furuno et al., 1999) was cloned into pcDNA3 (Invitrogen). Myc-tagged cyclin A was linked via an AGAEF linker to a cyan fluorescent protein (CFP; CLONTECH Laboratories, Inc.) to give pcDNA3-myc-cyclin A–CFP. All other cDNA constructs containing point mutations and deletions of cyclin A were fused to MmGFP via an AGAEF linker. The cyclin A D-box (RAALAVLKS) was replaced with that of cyclin B1 (RTALGDIGN) to give pcDNA3-myc-B1 D-box-cyclin A–GFP; R^{47} of cyclin A was replaced with an alanine to give pcDNA3-myc-R47A cyclin A–GFP; the D-box of cyclin A was deleted (RT^{46}-G^{56}NP-) for pcDNA3-myc-ΔD-box cyclin A–GFP; R^{211} was replaced with an alanine to give pcDNA3-myc-MAAIL cyclin A–GFP; the NH_2-terminal 97 amino acids of cyclin A were replaced with a methionine residue to give ΔN97 cyclin A–GFP; and the amino acids COOH-terminal to A^{98} of cyclin A and ΔD-box cyclin A were removed to give pcDNA3-myc-1–98 cyclin A–GFP and pcDNA3-myc-1–98 ΔD-box cyclin A–GFP, respectively. pCMX-cyclin B1–yellow fluorescent protein (YFP) has been described previously (Hagting et al., 1999). pEF-Bub1-dominant negative was provided by Stephan Geley and Tim Hunt (Imperial Cancer Research Fund, London, UK). All plasmid preparations were resuspended in 10 mM Tris, pH 8.0, for microinjection.

Baculovirus expression constructs of cyclin A and $(His)_6$-Cdk2 have been described previously (Krude et al., 1997). Both MmGFP alone and the ΔN97 cyclin A–GFP construct were cloned downstream of glutathione *S*-transferase (GST) in pGEX-2T (Amersham Pharmacia Biotech). A GST-Cdk–activating kinase (CAK) construct was provided by Carl Mann (Commissariat à L'Energie Atomique [CEA], Saclay, France). An expression construct for GroEL and GroES was provided by Dr. George Banting (University of Bristol, Bristol, UK). Maps of all constructs are available on request.

Protein Expression and Purification and Histone H1 Kinase Assays

Cyclin A–$(His)_6$-Cdk2 and cyclin A-GFP–$(His)_6$-Cdk2 complexes and $(His)_6$-cyclin A–GFP and $(His)_6$-Cdk2 proteins were expressed in baculovirus-infected Sf9 cells and purified as described previously (Krude et al., 1997). Proteins were concentrated in 10 mM Hepes, pH 7.4, 150 mM NaCl, 1 mM EDTA using Vivaspin microconcentrators and stored as 10% glycerol stocks. GST-GFP, GST-ΔN97 cyclin A–GFP, and GST-CAK proteins were expressed in *Escherichia coli* BL21 and purified as described previously (Hagting et al., 1999). GST-ΔN97 cyclin A–GFP was coexpressed with GroEL and GroES. GFP and ΔN97 cyclin A–GFP were cleaved from GST with thrombin (Sigma-Aldrich) or Factor Xa (Novagen), respectively, and GST-CAK was eluted from glutathione-Sepharose (Amersham Pharmacia Biotech) according to the manufacturer's instructions. Factor Xa was removed from GFP protein preparations using Xarrest agarose (Novagen). GFP, ΔN97 cyclin A–GFP, and GST-CAK were concentrated in 12.5 mM Tris, pH 8.0, 200 mM NaCl, 2.5 mM DTT; 10 mM K_2HPO_4/KH_2PO_4, pH 7.2, 100 mM KCl; and 20 mM Tris, pH 8.0, 150 mM NaCl, 1 mM DTT, respectively. ΔN97 cyclin A–GFP preparations consisted of ~30% ΔN97 cyclin A–GFP protein and 70% chaperonin proteins. All other proteins were >90% pure on Coomassie-stained gels. Histone H1 kinase assays were performed as described previously (Krude et al., 1997).

Immunofluorescence

HeLa cells were seeded onto metasilicate-coated coverslips, then fixed and stained using paraformaldehyde/Triton as described (Pines, 1997). All antibodies were diluted in 3% BSA/PBS, and washes were carried out with 0.2% Tween 20/PBS. Rabbit polyclonal anticyclin A antibodies (Pines and Hunter, 1991), monoclonal anti–β-tubulin antibodies (Amersham Pharmacia Biotech), and polyclonal anti-Mad2 (Babco) antibodies were used at dilutions of 1:2,000, 1:200, and 1:200, respectively. Monoclonal anticentrosomal CTR453 serum (a gift of Dr. Michel Bornens, Institut Curie, Paris, France) was used undiluted. Secondary antibodies (Jackson ImmunoResearch Laboratories) were diluted 1:200. Coverslips were mounted in 0.1% 1,4-phenylenediamine, 90% glycerol in PBS, pH 9.0, containing 50 nM TOTO-3 iodide (Molecular Probes). Cells were analyzed by confocal laser scanning microscopy. Z-series of images were projected using Lasersharp software (Bio-Rad Laboratories) and exported to Adobe Photoshop®.

Microinjection and Time-Lapse Imaging and Analysis

Cells were analyzed by time-lapse DIC-fluorescence microscopy as described previously (Clute and Pines, 1999; Furuno et al., 1999). For comparative quantitative analyses, all parameters were fixed: a fluorescence exposure time of 200 ms, a 40× oil objective with a numerical aperture of 1.0, and an image bin size of 4 were used. Images were saved in IPLab Spectrum format as unsigned 16 data using a reference look up table with a preset linear pixel intensity scale. IPLab Spectrum was used to quantify the amount of fluorescence as described previously (Clute and Pines, 1999; Furuno et al., 1999). DIC images were used to determine mitotic phases. Images were converted to PICT format and exported to Adobe Photoshop®.

Quantification of Cyclin A–GFP Protein Levels In Vivo

To determine the fluorescence per mole of GFP, glass needles of fixed diameter were filled with serial dilutions of GFP protein containing 1 mg/ml BSA,

images were taken as described by Howell et al. (2000), and the fluorescence and volume of needles were quantified using IPLab Spectrum software. To quantify the amount of endogenous cyclin A in late G2 phase cells, HeLa cells were synchronized in late G2 phase according to Tobey et al. (1990) and known numbers of cells were immunoblotted against fixed amounts of cyclin A–GFP standard. Bands were quantified using NIH Image v1.61 software.

Online Supplemental Material

The levels of cyclin A in late G2 phase cells were quantified as described in Materials and Methods. Two separate late G2 phase cell populations, each immunoblotted in duplicate, were used. To distinguish YFP from CFP fluorescence, custom-designed filter sets (JP4; Chroma Technology) were used. To ensure that there were no bleed-through effects, fluorescence images were taken of HeLa cells microinjected with cytomegalovirus promotor-driven cDNA constructs encoding either cyclin A–CFP or cyclin B1–YFP. Identical microscope and camera settings and an exposure time of 250 ms were used for all images. To determine the effect of 1% DMSO on the duration of mitosis phases, HeLa cells were synchronized in late G2 phase and followed by time-lapse microscopy either in the presence or absence of 1% DMSO. These results are available at http://www.jcb.org/cgi/content/full/153/1/121/DC1.

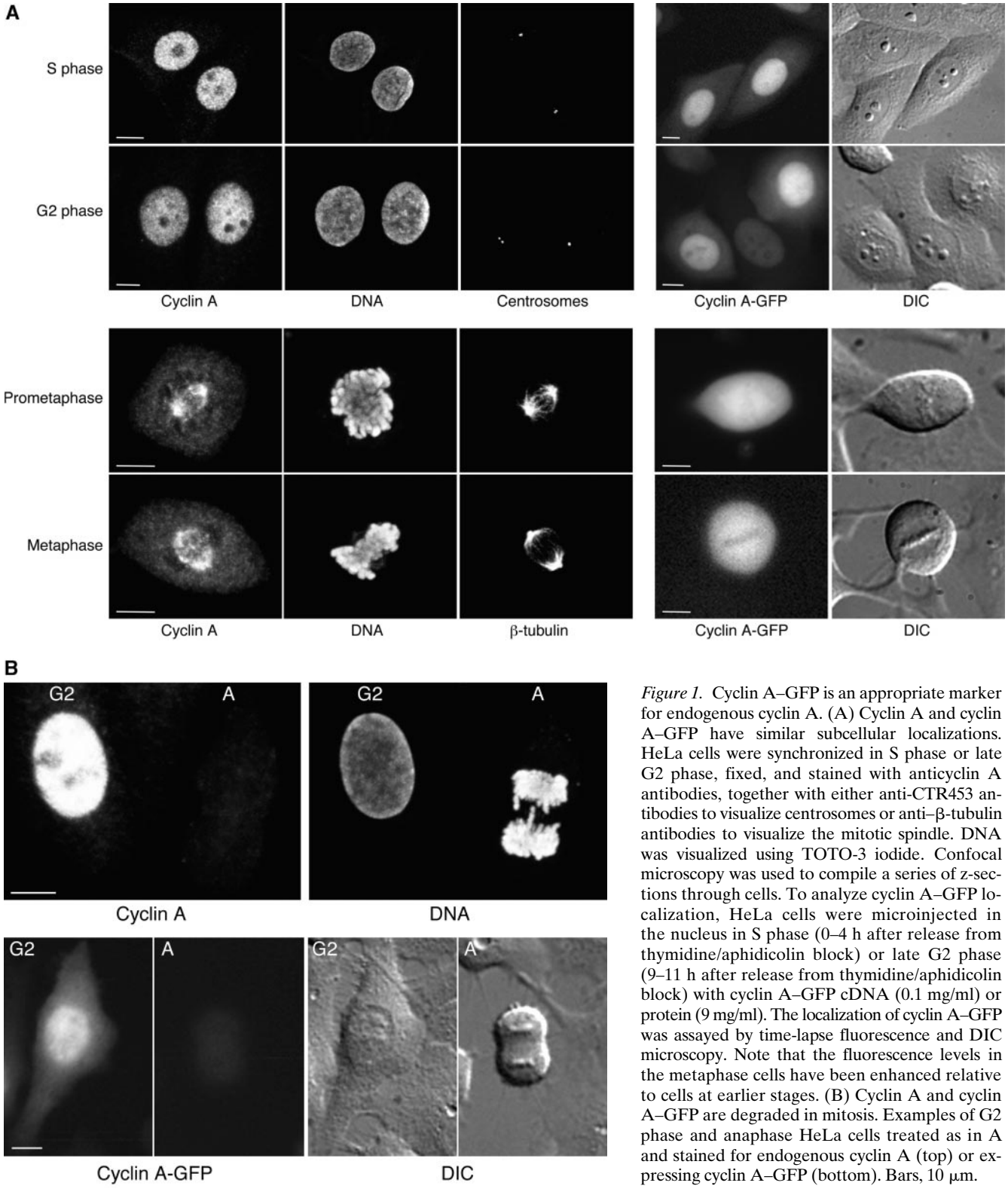

Figure 1. Cyclin A–GFP is an appropriate marker for endogenous cyclin A. (A) Cyclin A and cyclin A–GFP have similar subcellular localizations. HeLa cells were synchronized in S phase or late G2 phase, fixed, and stained with anticyclin A antibodies, together with either anti-CTR453 antibodies to visualize centrosomes or anti–β-tubulin antibodies to visualize the mitotic spindle. DNA was visualized using TOTO-3 iodide. Confocal microscopy was used to compile a series of z-sections through cells. To analyze cyclin A–GFP localization, HeLa cells were microinjected in the nucleus in S phase (0–4 h after release from thymidine/aphidicolin block) or late G2 phase (9–11 h after release from thymidine/aphidicolin block) with cyclin A–GFP cDNA (0.1 mg/ml) or protein (9 mg/ml). The localization of cyclin A–GFP was assayed by time-lapse fluorescence and DIC microscopy. Note that the fluorescence levels in the metaphase cells have been enhanced relative to cells at earlier stages. (B) Cyclin A and cyclin A–GFP are degraded in mitosis. Examples of G2 phase and anaphase HeLa cells treated as in A and stained for endogenous cyclin A (top) or expressing cyclin A–GFP (bottom). Bars, 10 μm.

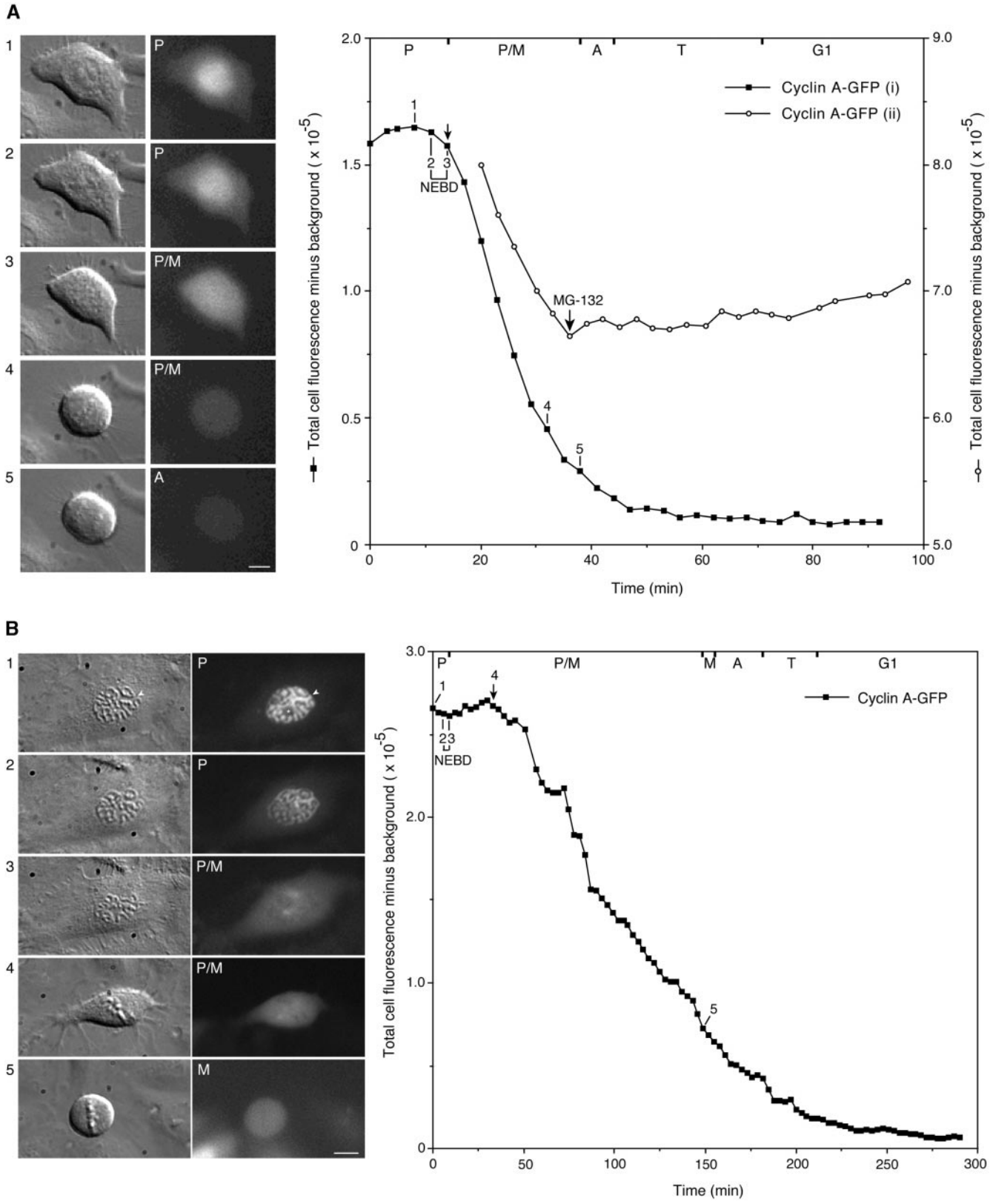

Results

Cyclin A–GFP Is a Valid Marker for Endogenous Cyclin A

Although cyclin A was known to be degraded before cyclin B, the precise timing of cyclin A degradation was unclear. Therefore, we analyzed cyclin A degradation in real time using cyclin A–GFP fusion proteins (the somatic form of human cyclin A, sometimes called cyclin A2). We have validated previously a cyclin B1–GFP fusion protein to analyze the in vivo degradation of human cyclin B1 (Clute and Pines, 1999), but we carefully characterized the cyclin A–GFP fusion protein to ensure that it was an appropriate marker for endogenous cyclin A.

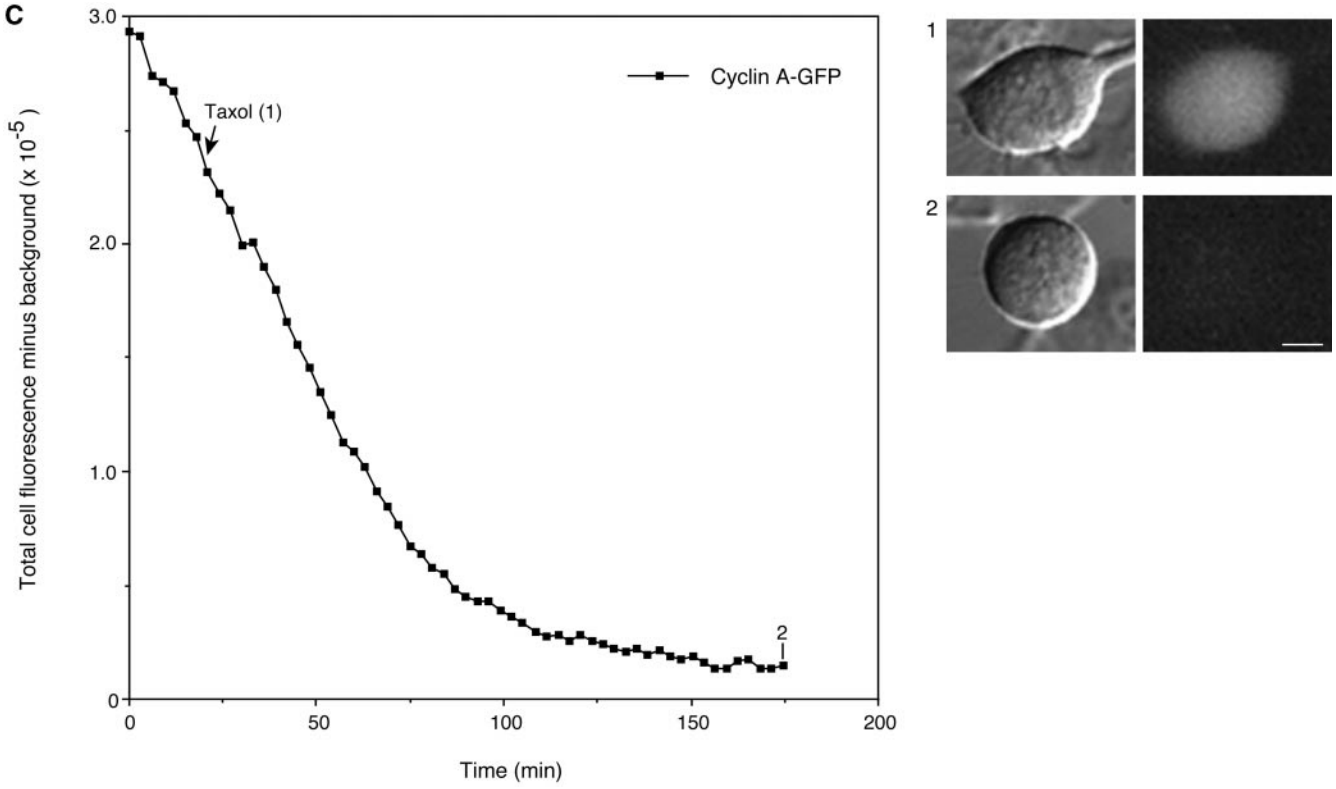

Figure 2. Cyclin A is degraded from early prometaphase by a 26S proteasome-dependent pathway and is not inhibited by the spindle checkpoint. (A) Cyclin A begins to be degraded in prometaphase. HeLa cells synchronized in late G2 phase were microinjected in the nucleus with cyclin A–GFP protein (9 mg/ml), and followed by time-lapse fluorescence and DIC microscopy. Images (200-ms exposure) were taken at 3-min intervals. The total cell fluorescence minus background was quantified for each cell in successive images of a time series and plotted over time. A graph of a single cell (■), representative of 42 cells analyzed, is shown. The start and finish of NEBD are marked and an arrow shows the time at which fluorescence levels began to decrease. The stages of mitosis are indicated at the top of the figure. Because metaphase is relatively short and variable in HeLa cells (9.9 ± 9.6 min in uninjected cells, $n = 42$) and images were only taken at 3-min intervals, in some cells (including the cell shown here) metaphase was not observed. Another cell was similarly injected and analyzed, but was treated with the 26S proteasome inhibitor MG-132 (100 μM; Calbiochem) during prometaphase. This cell remained in prometaphase for the duration of the experiment (data not shown). The graph shown (○) is representative of three cells analyzed. P, prophase; P/M, prometaphase; A, anaphase; T, telophase; G1, G1 phase. (B) Cyclin A begins to be degraded just after NEBD in PtK_1 cells. Prophase PtK_1 cells were microinjected with cyclin A–GFP protein (9 mg/ml) and analyzed as in A. A graph of a single cell, representative of nine cells analyzed, is shown. The initiation and completion of NEBD are marked and an arrow shows the time at which fluorescence levels began to decrease. The white arrowhead shows the localization of cyclin A–GFP between condensing chromosomes in prophase, and an asterisk indicates the original position of the nucleolus. M, metaphase. (C) Cyclin A–GFP is still degraded in the presence of taxol. HeLa cells synchronized in late G2 phase were injected with cyclin A–GFP protein and analyzed as above. Once in prometaphase, cells were treated with 10 μM taxol (Sigma-Aldrich). The degradation profile of a single cell, representative of four cells analyzed, is shown. DIC and fluorescence images show that cyclin A–GFP was completely degraded and that the cell remained in prometaphase for the duration of the experiment. Bars, 10 μm.

First, we determined that cyclin A–GFP bound and activated Cdk2 with similar efficiency to wild-type cyclin A; cyclin A–GFP stimulated the histone H1 kinase activity of Cdk2 to 111% of the level achieved by an equivalent amount of wild-type cyclin A. Monomeric Cdk2 had <0.6% of the activity of cyclin A/Cdk2. To analyze the subcellular localization of cyclin A–GFP during the cell cycle, HeLa cells were microinjected in S or G2 phase with cyclin A–GFP cDNA or purified protein, and followed by time-lapse fluorescence and DIC microscopy (Fig. 1 A). These images were compared with cells stained with anticyclin A antibodies, together with anti-CTR453 centrosomal antibodies or anti–β-tubulin antibodies, and with a DNA stain (Fig. 1 A). Cyclin A–GFP mimicked the localization of endogenous cyclin A at each stage of the cell cycle. During S and G2 phases, cyclin A and cyclin A–GFP were nuclear and excluded from the nucleoli; both also stained the centrosomes from early prophase onwards, in agreement with previous reports (Pines and Hunter, 1991; Bailly et al., 1992; Pagano et al., 1992; Girard et al., 1995). From prophase, cyclin A and cyclin A–GFP became excluded from the condensing chromosomes in the nucleus. In prometaphase and metaphase, endogenous cyclin A and cyclin A–GFP were distributed throughout the cell and concentrated at the mitotic spindle.

Finally, we analyzed the stability of cyclin A–GFP through the cell cycle. Like endogenous human cyclin A (Pines and Hunter, 1990), cyclin A–GFP was stable in S and G2 phases (Furuno et al., 1999). During mitosis, cyclin A–GFP fluorescence rapidly decreased (Fig. 1 B), consistent with the degradation of endogenous cyclin A (Fig. 1 B). This decrease in cyclin A–GFP levels during mitosis was conferred by cyclin A rather than GFP, because GFP was stable throughout mitosis (data not shown).

Cyclin A–GFP Is Degraded from Early Prometaphase

To determine when cyclin A–GFP proteolysis was initiated, HeLa cells were microinjected with cyclin A–GFP protein and followed at 3-min intervals by time-lapse fluorescence

Table I. Degradation Rates of Cyclin A–GFP D-Box Mutants

Construct		Rate of degradation (mean ± SD)
	n	min^{-1}
Cyclin A–GFP	13	19,926 ± 5,611
Cyclin B1 D-box–cyclin A-GFP	6	17,961 ± 4,266
R47A cyclin A–GFP	3	19,316 ± 5,495
ΔD-box cyclin A–GFP	10	20,604 ± 4,682

Degradation rates were calculated from the linear part of the graphs plotted for the decrease in fluorescence.

and DIC microscopy. The total fluorescence, i.e., the amount of cyclin A–GFP, in individual cells was quantified and plotted over time. Cyclin A–GFP protein levels consistently began to fall just after the start of NEBD, reaching very low levels by the time chromosomes aligned (Fig. 2 A). Equivalent results were obtained when cells were injected with a cDNA expression construct rather than purified protein (data not shown). The rapid decrease in cyclin A–GFP levels required 26S proteasome-mediated degradation because it was blocked by the proteasome inhibitor MG-132 (Fig. 2 A).

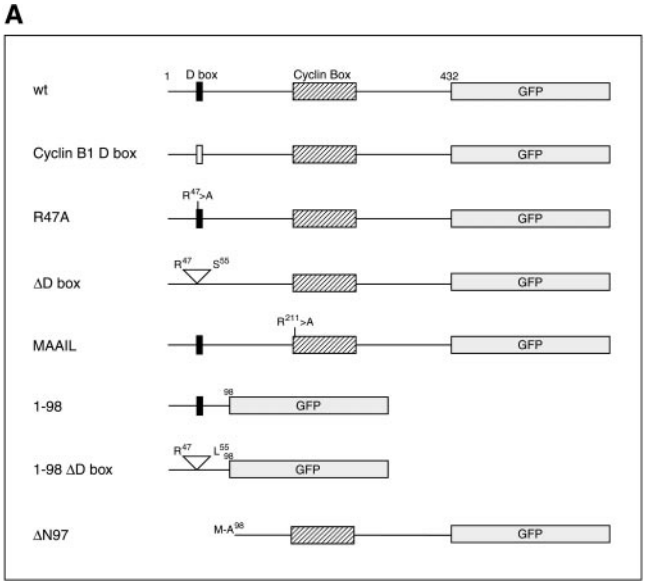

Figure 3. Cyclin A–GFP degradation is D-box independent and temporally regulated by Cdk binding. (A) Schematic diagram of cyclin A–GFP constructs. The D-box and cyclin box of human cyclin A and GFP are indicated. In the cyclin B1 D-box construct, the D-box of cyclin A has been replaced with that of cyclin B1. The R47A and ΔD-box constructs do not contain a functional D-box. MAAIL and 1–98 constructs are non-Cdk binding forms of cyclin A–GFP. The ΔN97 protein begins with a methionine, followed by amino acid 98 of cyclin A. (B–G) Degradation profiles of the cyclin A–GFP constructs in A. HeLa cells synchronized in late G2 phase were microinjected with cytomegalovirus promotor-driven cDNAs (0.1 mg/ml) and followed by time-lapse fluorescence and DIC microscopy at 3 min intervals. The total cell fluorescence minus background was quantified for each cell and plotted over time. A representative graph, together with the total number of cells analyzed, is shown for each construct. The stages of mitosis are indicated at the top of each figure. In G the stages of mitosis for the two different constructs are shown. For some cells, no obvious metaphase was observed. NEBD initiation and completion or chromosome segregation are marked. Arrows indicate the times at which fluorescence levels began to decrease.

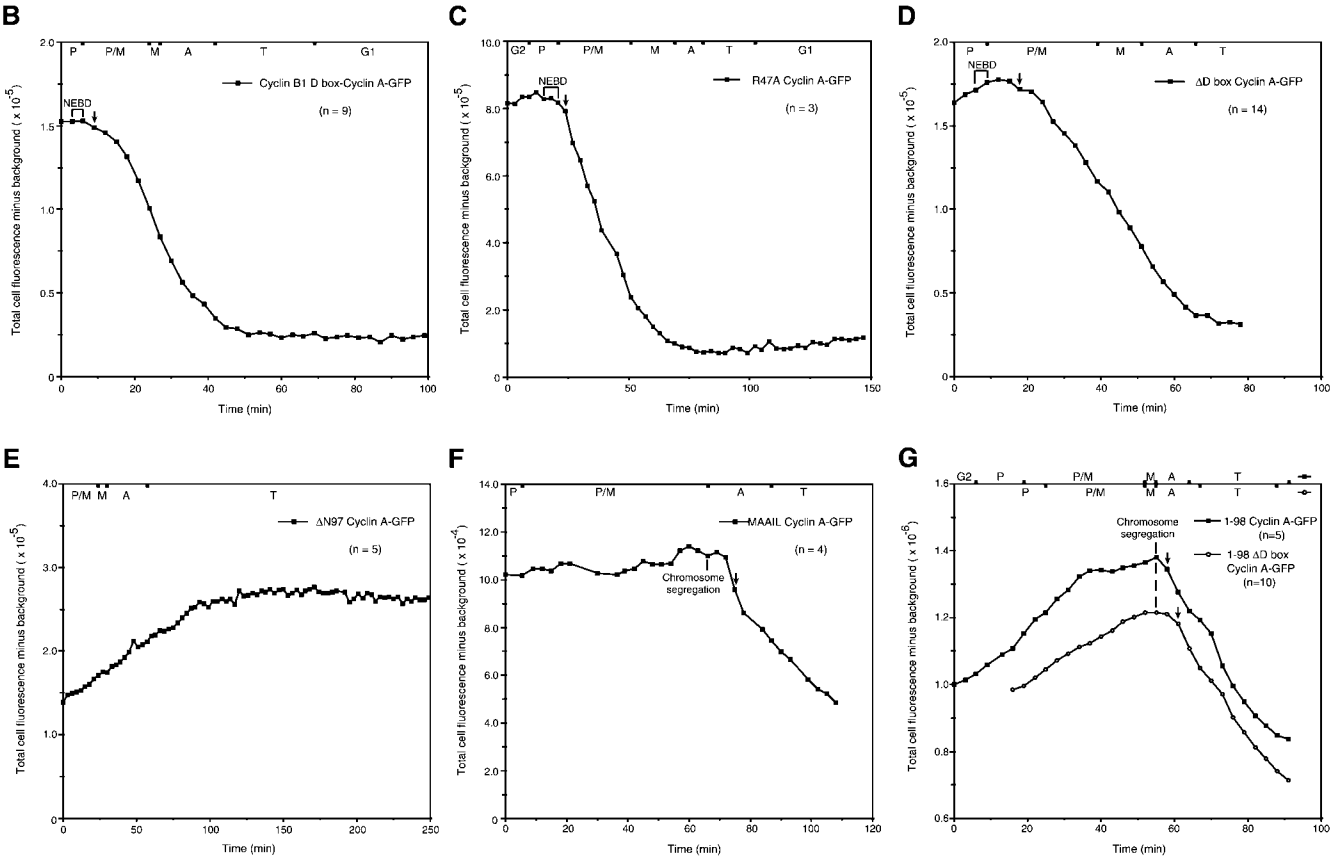

To determine more precisely when cyclin A–GFP degradation began, data were collated for the time in relation to NEBD at which cyclin A–GFP levels began to decrease. (We injected cyclin A–GFP protein rather than cDNA to avoid any possible lag in the decrease of cyclin A–GFP levels due to mRNA translation.) NEBD observed by DIC correlated with the redistribution of cyclin A–GFP between the cytoplasm and nucleus. Thus, we defined the initiation of NEBD as the time when the amount of cyclin A–GFP fluorescence in the cytoplasm increased and that in the nucleus decreased (NEBD was considered complete when cyclin A–GFP fluorescence was equally distributed throughout the cell). This analysis showed that cyclin A–GFP protein levels decreased 0–9 min (average 5.4 ± 3.2 min) after the initiation of NEBD (n = 20) (metaphase occurred 15–51 min after NEBD, average 26 ± 9.5 min, in uninjected HeLa cells [n = 37]). Cyclin A–GFP levels never decreased before NEBD began.

It had been reported that cyclin A degradation occurred during anaphase in nontransformed mammalian cells and thus was delayed compared with transformed cells (Girard et al., 1995). Therefore, we compared the degradation of cyclin A–GFP in HeLa cells to that in the nontransformed cell line PtK_1. The level of cyclin A–GFP fluorescence also decreased from early prometaphase in PtK_1 cells (Fig. 2 B) in a very similar manner to HeLa cells.

In prometaphase, chromosomes stochastically attach to the mitotic spindle and congress to the cell equator. During this time, chromosomes that are not attached to both poles activate the spindle checkpoint, preventing both cyclin B1 and securin from being degraded and thereby inhibit anaphase. Given that cyclin A–GFP was degraded during prometaphase and that human cyclin A is unstable in nocodazole-treated cells (Pines and Hunter, 1990; Pagano et al., 1992), we predicted that prolonged activation of the spindle checkpoint with a spindle poison should not affect the kinetics of cyclin A–GFP degradation. To test this, prometaphase cells that were degrading cyclin A–GFP were treated with taxol (Fig. 2 C). These cells remained in prometaphase for >2 h, long after chromosome alignment is usually achieved, showing that the spindle checkpoint was fully active, but this had no effect on cyclin A–GFP degradation.

Cyclin A–GFP Degradation Is D-Box Independent and Regulated by Cdk Binding

To analyze how cyclin A degradation was initiated in early prometaphase, before the metaphase degradation of cyclin B1, we attempted to change the timing of cyclin A destruction by replacing the D-box of cyclin A with that of cyclin B1 (Fig. 3 A). However, this had no effect on cyclin A–GFP degradation; the protein levels still decreased just after NEBD (Fig. 3 B). Moreover, the rate of degradation of cyclin B1-D-box–cyclin A-GFP was similar to that of wild-type cyclin A–GFP (Table I).

To determine whether the D-box was necessary for the prometaphase degradation of cyclin A, constructs were made either with the R47A mutation that perturbs D-box function (Glotzer et al., 1991) or completely lacking the D-box (Fig. 3 A). Both these mutant proteins were degraded with the same timing and rate as wild-type cyclin A–GFP (Fig. 3, C and D, and Table I). We were able to stabilize cyclin A in vivo by removing the first 97 amino acids of human cyclin A, including the D-box and the adjacent lysine-rich region (Fig. 3 E).

Cdk binding had been shown to be required for the degradation of *Xenopus* cyclin A in vitro (Stewart et al., 1994). To analyze whether this altered its degradation properties in vivo, we made an R→A mutation in the MRAIL motif of the cyclin box (MAAIL), or used just the first 98 amino acids of cyclin A with, or without, the D-box (Fig. 3 A). None of these mutants were able to bind to Cdk2 (data not shown; Stewart et al., 1994), but all were degraded in mitosis in vivo (Fig. 3, F and G). However, this degradation was delayed because protein levels did not fall until sister chromatid segregation. Thus, although Cdk binding was not required for the degradation of cyclin A–GFP, it did influence the timing of its destruction.

Overexpression of Cyclin A–GFP Delays Chromosome Alignment and Anaphase Onset

Time-lapse analyses indicated that cyclin A may need to be degraded in prometaphase to enable chromosomes to align. Uninjected HeLa cells took an average of 26 ± 9.5 min from the beginning of prometaphase (completion of NEBD) to the alignment of chromosomes at the metaphase plate (n = 37). However, increasing the amount of cyclin A–GFP increased the time between NEBD and stable chromosome alignment or anaphase (up to >500 min). During this delay, chromosomes would sometimes appear to align at the cell equator, but would always become misaligned again in subsequent images (see below). To confirm the effect of cyclin A–GFP overexpression on chromosome alignment, we examined this in PtK_1 cells. Consistent with Rieder et al. (1994), we found that uninjected PtK_1 cells took an average of 27 ± 7.5 min from the start of prometaphase to chromosome alignment (n = 15). But this period was extended to as long as 405 min in PtK_1 cells microinjected with increasing amounts of cyclin A–GFP. This mitotic delay induced by overexpressing cyclin A was not due to premature mitosis, because the delay still occurred in PtK_1 cells that were injected with cyclin A–GFP protein in prophase. Overexpressing cyclin A–GFP in either PtK_1 or HeLa cells had no effect on the duration of prophase, anaphase or telophase (data not shown).

To ensure that the delay in chromosome alignment induced by cyclin A–GFP was not a result of the GFP tag, we overexpressed untagged cyclin A with GFP as an injection marker. Overexpressing wild-type cyclin A also caused a delay in stable chromosome alignment and anaphase (Fig. 4 A), whereas GFP alone had no effect on mitosis (data not shown).

Given that cyclin A was normally degraded during prometaphase, the delay in chromosome alignment and anaphase caused by increased amounts of cyclin A might have been due to a delay in its removal. In agreement with this, we found that there was a linear relationship between the period of time from NEBD completion to chromosome alignment and the amount of cyclin A–GFP protein present in cells at NEBD (Fig. 4 B). Cells in which the time from NEBD completion to chromosome alignment was >50 min had a statistically significant delay in chromosome alignment compared with uninjected cells (significance level = 99%). Using the line of best fit, the minimum amount of cy-

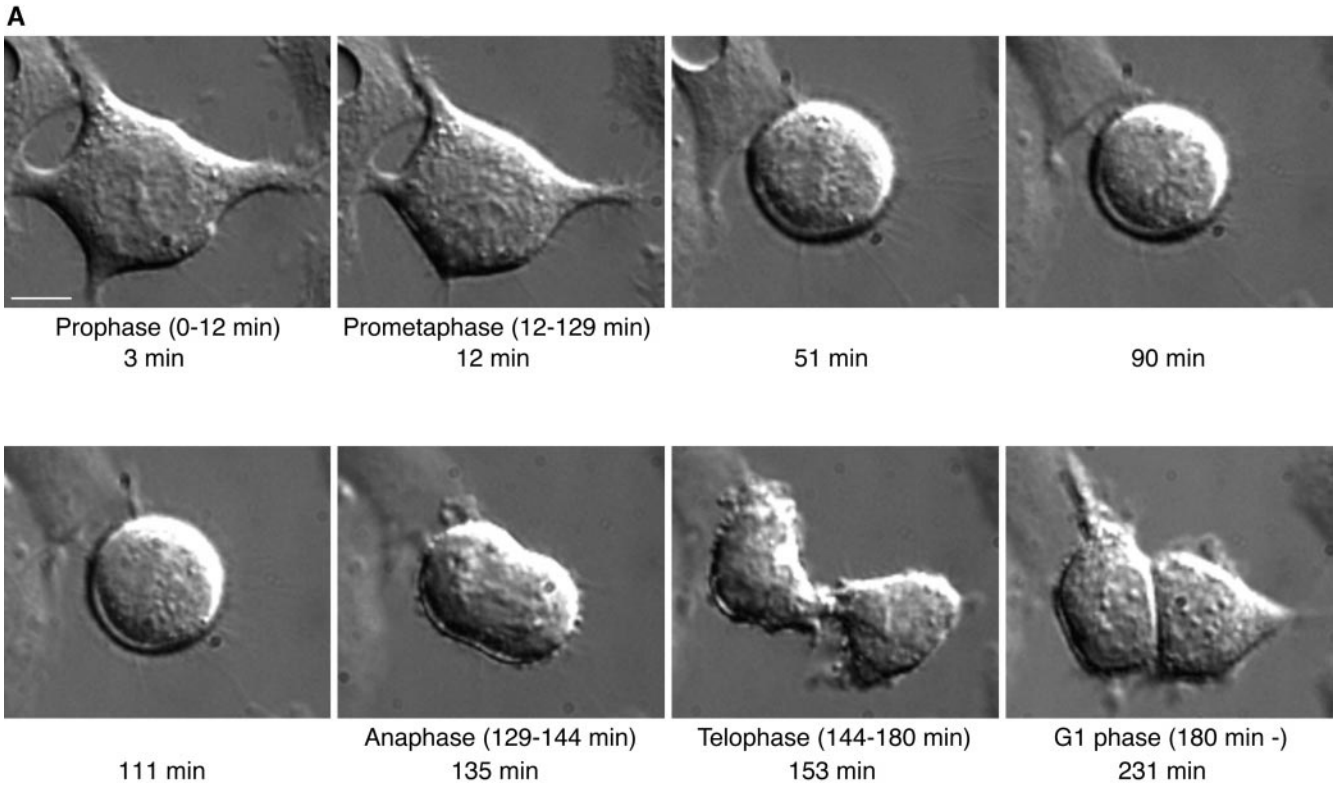

Figure 4. Cyclin A delays chromosome alignment and anaphase in a concentration-dependent manner. (A) Overexpression of wild-type cyclin A delays chromosome alignment. Late G2 phase HeLa cells were microinjected with cyclin A and GFP expression constructs. DIC images were taken at 3-min intervals. A cell in which the period of time from NEBD completion to chromosome alignment was prolonged (117 min) compared with uninjected cells (26 ± 9.5 min, $n = 37$) is shown and is representative of 5 out of 15 cells analyzed. The duration of each mitotic phase is indicated. (B) Concentration dependence of the cyclin A–induced delay. HeLa cells were microinjected in late G2 phase with cyclin A–GFP protein and followed by time-lapse fluorescence and DIC microscopy at 3 min intervals. Identical microscope and camera settings were used in all experiments and the time from the completion of NEBD to chromosome alignment was plotted against the total cell fluorescence minus background at NEBD (before cyclin A–GFP degradation) for each cell. For cells where stable chromosome alignment was not observed, the duration from NEBD to sister chromatid segregation was measured. The average period from completion of NEBD to chromosome alignment in uninjected HeLa cells (26 ± 9.5 min, $n = 37$) is indicated by a black square with error bars. Prometaphase was statistically prolonged compared with uninjected cells (significance level = 99%) in those cells with periods from NEBD completion to chromosome alignment >50 min (indicated by a dashed line). The amount of cyclin A–GFP is also given in units (x) equivalent to the amount of endogenous cyclin A in a late G2 cell (see Materials and Methods). (C) Chromosome alignment is delayed by MG-132. HeLa cells were treated in prophase (time 0) with 100 μM MG-132 (Calbiochem) to inhibit 26S proteasome-mediated degradation, and DIC images were taken at 3 min intervals. 1 cell, representative of 10 cells analyzed, is shown. NEBD was complete within 7 min, but chromosomes remained misaligned 160 min later. DMSO alone had no effect (data not shown). Bars, 10 μm.

clin A–GFP required to cause a delay in chromosome alignment corresponded to a fluorescence of 10^6, equivalent to half the amount of endogenous cyclin A in a late G2 phase cell, i.e., a 1.5-fold increase in the total amount of cyclin A. Furthermore, data from those cells with a delay in chromosome alignment ($n = 10$) showed that cyclin A–GFP levels consistently fell to a threshold level of $(3.6 \pm 2.8) \times 10^5$ (equivalent to ~1/5 the amount of endogenous cyclin A in late G2 phase) before chromosomes could align. This indicated that the delay in chromosome alignment and anaphase could occur under physiological conditions.

Our results indicated that cyclin A, or another protein(s) with which it competed for the degradation machinery, had to be removed in prometaphase in order for

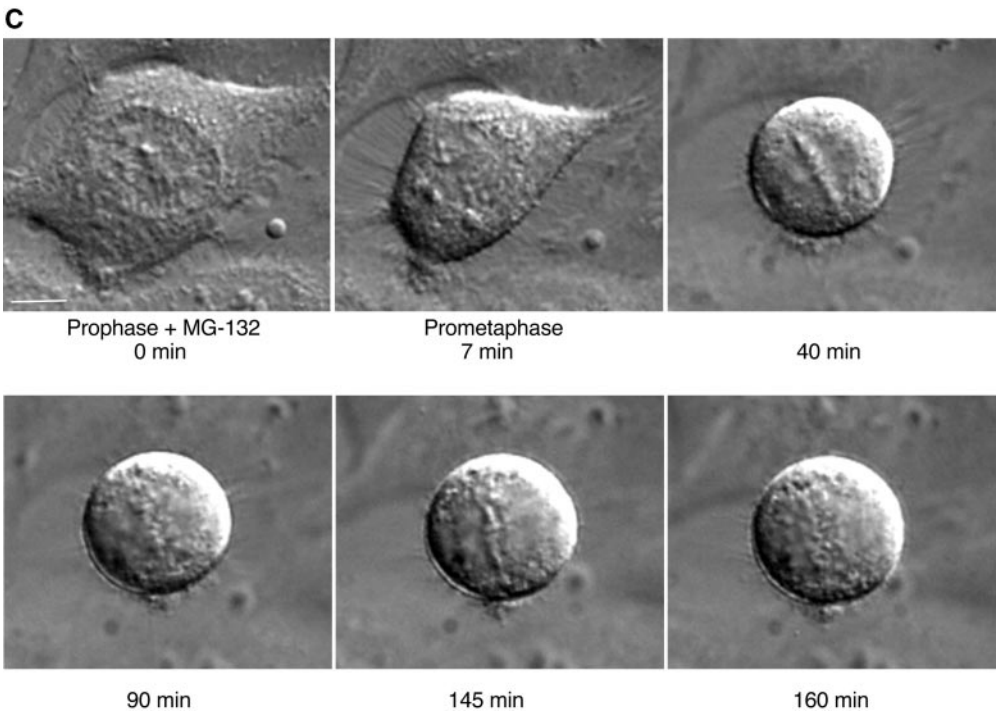

Figure 4 (continued)

chromosomes to align. To confirm this in cells with physiological levels of cyclin A, we inhibited ubiquitin-mediated degradation in prometaphase with MG-132 (Fig. 4 C). This caused cells to arrest with a phenotype similar to that of cells overexpressing cyclin A, i.e., individual chromosomes continuously moved to and from the cell equator and stable chromosome alignment was never achieved.

Cyclin A-GFP–induced Mitotic Delay Does Not Act via the Spindle Checkpoint

One means to prevent the alignment of chromosomes at the cell equator would be to perturb their bipolar attachment to the mitotic spindle. This would also activate the spindle checkpoint and prevent anaphase. To test whether the cyclin A–induced delay in chromosome alignment and anaphase correlated with activating the spindle checkpoint, we stained cells for the checkpoint protein Mad2. Mad2 localizes to kinetochores that are not attached to the mitotic spindle (Chen et al., 1996; Li and Benezra, 1996) and this is thought to correlate with an active checkpoint. Cells were microinjected with cyclin A–GFP cDNA and those that had not aligned their chromosomes 50 min after the completion of NEBD were scored as having a cyclin A-GFP–induced delay and were fixed and stained for Mad2. Mad2 did not localize to the kinetochores in any cells with a cyclin A-GFP–induced delay (Fig. 5 A).

To test further whether the spindle checkpoint was active during the cyclin A–induced mitotic delay, we analyzed the degradation of cyclin B1, which is inhibited by the spindle checkpoint. Human cyclin B1 tagged with YFP and cyclin A tagged with CFP were coexpressed in late G2 phase HeLa cells. Using custom-designed filter sets, the fluorescence levels of cyclin A–CFP and cyclin B1–YFP were followed independently in the same cell. This showed that cyclin B1–YFP was degraded during the cyclin A–CFP-induced mitotic delay (Fig. 5 B). As a further indication for whether the spindle checkpoint was required for the cyclin A–induced delay, we introduced a dominant negative form of Bub1 to inactivate the checkpoint. Bub1 is an essential component of the spindle checkpoint and a dominant negative form of this protein prevents cells from arresting in mitosis in response to nocodazole (Taylor and McKeon, 1997). Cells expressing dominant negative Bub1 entered anaphase prematurely (Fig. 5 C), in agreement with studies in which anti-Mad2 antibodies were used to inactivate the checkpoint (Gorbsky et al., 1998). However, dominant negative Bub1 did not abrogate the delay in chromosome alignment and anaphase caused by overexpressing cyclin A (Fig. 5 C). Finally, we added taxol to activate the spindle checkpoint in cells overexpressing cyclin A and B1. Taxol stabilized cyclin B1 and not cyclin A, in agreement with our previous results, but we found that cyclin B1 only became stable once cyclin A had fallen below a threshold amount (Fig. 5 D). Before this point, cyclin B1 continued to be degraded even in the presence of taxol, indicating that excess cyclin A may interfere with the spindle checkpoint signal.

The Mitotic Delay Induced by Cyclin A May Not Be Due to Its Associated Cdk Activity

The delay in chromosome alignment and anaphase caused by increased levels of cyclin A–GFP could have been due to cyclin A–associated Cdk activity. Alternatively, it may have resulted from competition between cyclin A and another mitotic regulator for a limiting component of the degradation machinery. We attempted to distinguish between these two possibilities using ΔN97 cyclin A–GFP which could not be degraded in vivo (Fig. 3 E), but could still stimulate Cdk2 histone H1 kinase activity to levels equivalent to that of cyclin A–GFP (87% of wild-type cyclin A). If the delay caused by cyclin A was due to its associated Cdk activity, then expressing the nondegradable ΔN97 cyclin A–GFP at

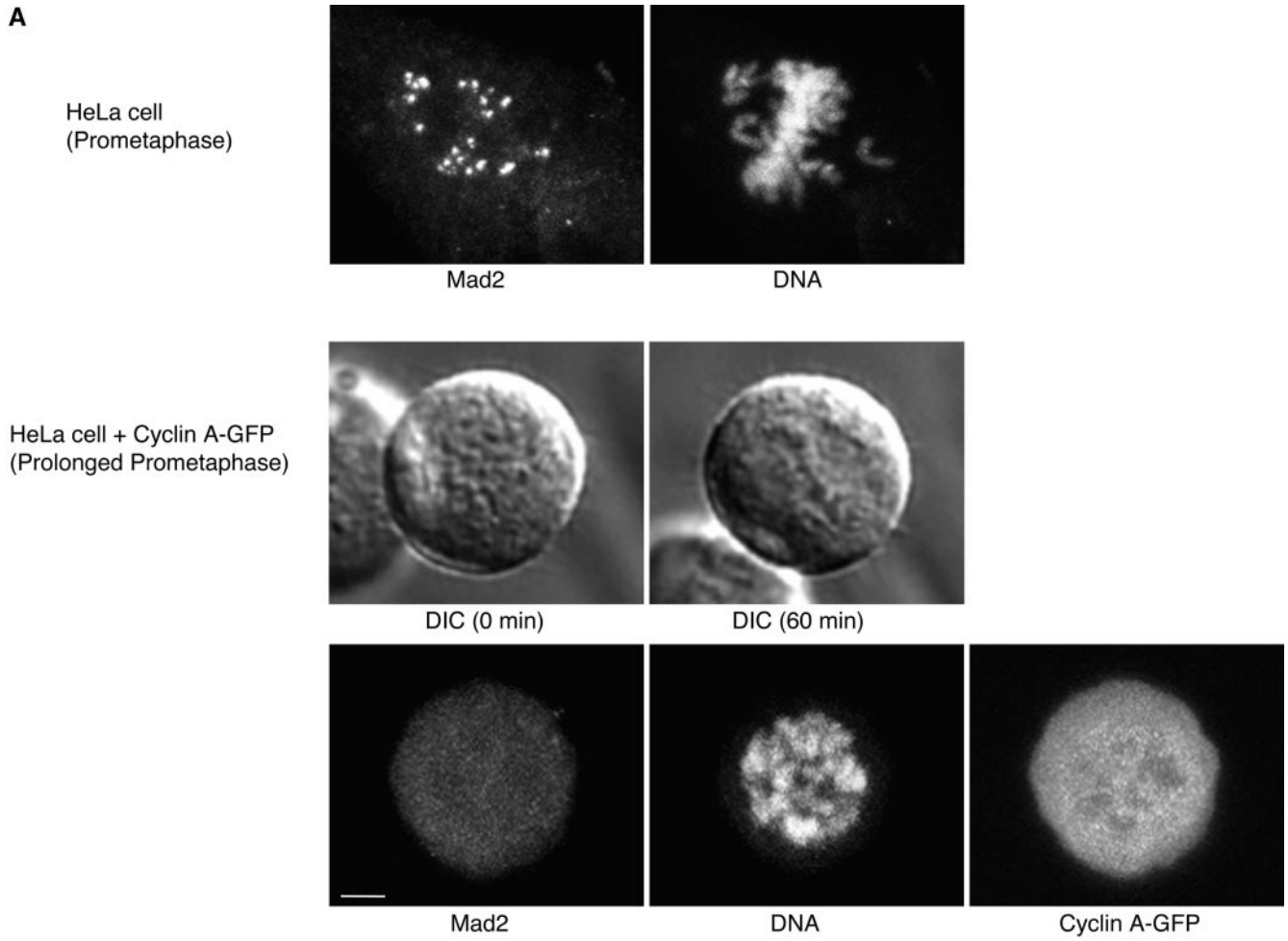

levels above the threshold amount (3.6×10^5) of cyclin A–GFP required to prevent chromosome alignment should result in an arrest before chromosome alignment. However, this was not observed. Instead, cells aligned their chromosomes normally, but arrested in either anaphase or telophase (Fig. 6). With high levels of ΔN97 cyclin A–GFP, cells underwent anaphase A and often anaphase B. Sometimes a cleavage furrow formed, but this usually retracted and chromosomes cycled back and forth between the cell equator and the spindle poles. With lower levels of ΔN97 cyclin A–GFP, cells underwent a normal anaphase and cytokinesis, but arrested in telophase with condensed chromosomes

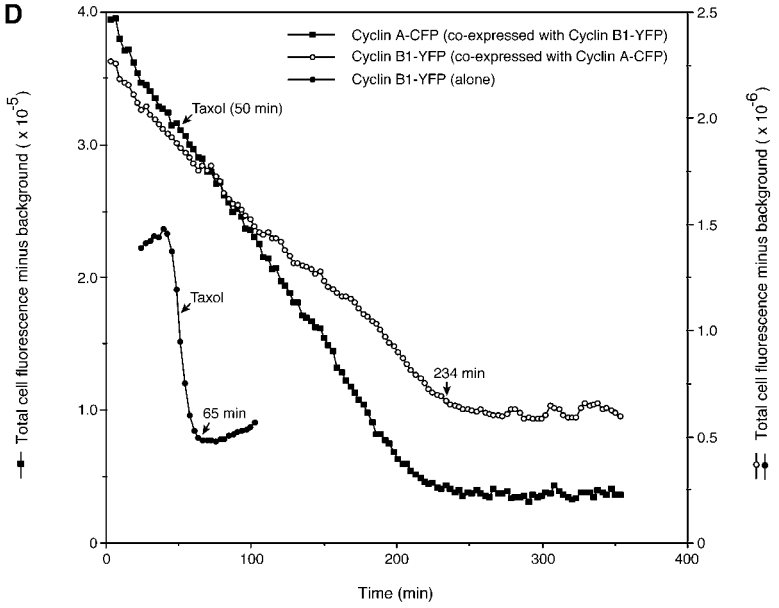

Figure 5. The delay in chromosome alignment and anaphase does not correlate with an active spindle checkpoint. (A) Mad2 is not on kinetochores in cells delayed by cyclin A–GFP. HeLa cells expressing cyclin A–GFP cDNA were followed by time-lapse microscopy. Cells that had not aligned their chromosomes >50 min after NEBD were scored as having a cyclin A–GFP-induced delay, and were fixed and stained with anti-Mad2 antibodies and TOTO-3 iodide. DIC images were taken before fixation. Fluorescence images were compiled from a series of z sections through cells. 1 cell, representative of 11 cells analyzed, is shown. (B) Cyclin B1–YFP is degraded in cells delayed by cyclin A–CFP. HeLa cells synchronized in late G2 phase were coinjected with cyclin A–CFP and cyclin B1–YFP expression vectors. Cells were followed by time-lapse microscopy at 3-min intervals using custom-designed filter sets to discriminate CFP fluorescence from YFP fluorescence. The total cell fluorescence minus background was quantified independently for cyclin A–CFP and cyclin B1–YFP and plotted over time. Graphs from a cell with a cyclin A–CFP-induced delay in chromosome alignment and anaphase onset, representative of seven delayed cells analyzed, are shown. Initiation and completion of NEBD and chromosome segregation are marked. Chromosomes did not segregate until 187 min, 172 min after the completion of NEBD. Arrows indicate the time points at which cyclin A–CFP and cyclin B1–YFP fluorescence levels began to decrease (30 and 63 min, respectively). (C) Dominant negative Bub1 does not abrogate the cyclin A–induced delay. HeLa cells synchronized in late G2 phase were coinjected with cDNAs encoding dominant negative Bub1 and either GFP or cyclin A–GFP, and followed by time-lapse fluorescence and DIC microscopy. NEBD completion to chromosome segregation took 36 ± 8.9 min in uninjected cells (n = 46), but significantly less time (<13 min, significance level = 99%) in cells expressing Bub1 DN and GFP at a fluorescence $\geq 10^6$ (n = 11). In five out of nine cells coexpressing cyclin A–GFP and Bub1 DN at levels $>10^6$ (the level of cyclin A–GFP required to cause a delay in chromosome alignment in Fig. 4 B), NEBD to chromosome segregation was significantly prolonged compared with uninjected cells (>59 min). (D) Taxol does not stabilize cyclin B1 in cells with increased amounts of cyclin A. HeLa cells synchronized in late G2 phase were injected with cyclin B1–YFP alone or coinjected with cyclin A–CFP and cyclin B1–YFP expression constructs and followed as in B. Cells expressing cyclin B1–YFP cDNA alone were treated with taxol after cyclin B1–YFP degradation had commenced. The graph shown is representative of four such cells. Arrows indicate the timing of taxol addition and the stabilization of cyclin B1–YFP. Cells coexpressing cyclin A–CFP and B1–YFP were treated with 10 μM taxol if they had not aligned their chromosomes within 50 min of NEBD. Graphs of a single cell, representative of seven cells analyzed, are shown. The cell remained in prometaphase for the duration of the experiment. Bar, 5 μm.

and no nuclear envelope. Some cells with very low levels of ΔN97 cyclin A–GFP proceeded through most of mitosis normally, but telophase was prolonged (data not shown).

Discussion

In this paper we have analyzed the degradation of the mitotic regulator cyclin A using a GFP fusion protein together with live cell imaging. Cyclin A–GFP is a valid live cell marker for endogenous cyclin A because it stimulates the histone H1 kinase activity of Cdk2, localizes correctly during the cell cycle, is stable in S and G2 phases, and is degraded in mitosis.

Early Prometaphase Degradation of Cyclin A: Implications for Its Mitotic Functions and Degradation Pathway

We find that cyclin A–GFP levels begin to decrease in HeLa cells in early prometaphase, 0–9 min after the initiation of NEBD. The majority of cyclin A–GFP has disappeared by the time chromosomes align at metaphase, consistent with immunofluorescence results for endogenous cyclin A. Cyclin A–GFP degradation also begins in early prometaphase in the nontransformed PtK_1 cell line. This is in contrast to findings from Girard et al. (1995) who used immunofluorescence to show that cyclin A degradation is delayed until anaphase in nontransformed cells. This contradiction might arise from the analyses of different cell lines, but is more likely to be because immunofluorescence can only determine when cyclin A has disappeared, rather than when degradation is initiated.

Because cyclin A is degraded from NEBD onwards, its mitotic function has probably been completed before NEBD, consistent with our observation that cyclin A becomes dispensable for mitosis ~10 min before NEBD (Furuno et al., 1999). The timing of cyclin A degradation in early prometaphase has important implications for the mechanism by which it is carried out. Cyclin A proteolysis is after cyclin B1/Cdk1 has been activated and translocated to the nucleus (Ookata et al., 1992; Furuno et al., 1999; Hagting et al., 1999), concordant with the requirement in vitro for cyclin B1/Cdk1 activity to trigger cyclin A degradation (Félix et al., 1990; Luca et al., 1991; Lorca et al., 1992b). We never observed cyclin A degradation before NEBD in HeLa or PtK_1 cells, indicating that NEBD itself may be required for cyclin A degradation, perhaps because components that are essential for proteolysis are sequestered in the cytoplasm.

The degradation of cyclin A during prometaphase presents a problem if it is mediated by the APC. Geley et al. (page 137) in this issue provide evidence that the APC is involved in the destruction of cyclin A; injecting antibod-

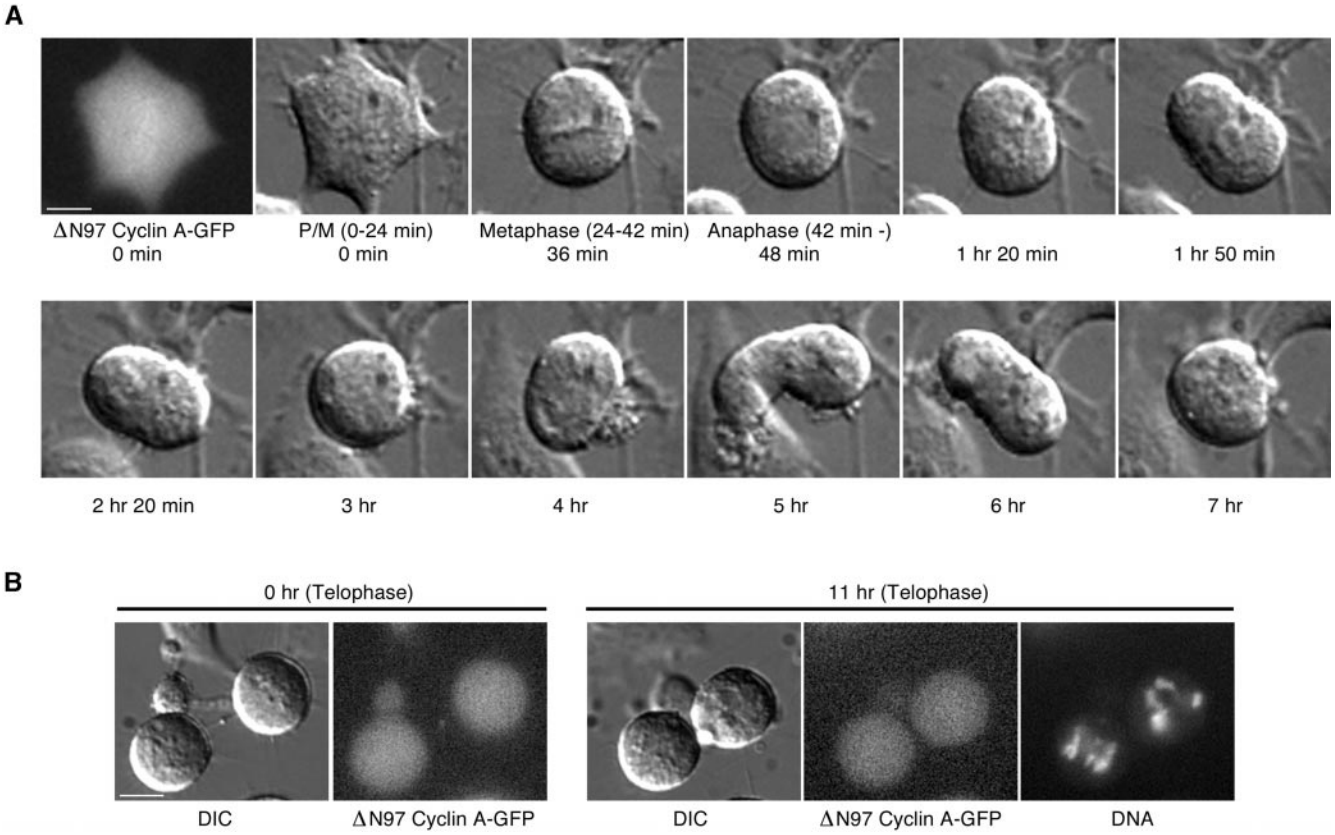

Figure 6. Nondegradable cyclin A–GFP does not prevent chromosome alignment, but arrests cells in anaphase or telophase. Late G2 phase HeLa cells were microinjected with a ΔN97 cyclin A–GFP expression vector and analyzed by time-lapse microscopy. Cells were scored as arrested if they remained in the same phase of mitosis for >3 h. Images of cells arrested in anaphase (A) or telophase (B) are shown. The DNA in cell B was stained by adding 1 μg/ml Hoechst 33342 (Sigma-Aldrich). Data are representative of 23 cells analyzed: 12 arrested in anaphase, 7 arrested in telophase and 4 cells with low levels of ΔN97 cyclin A–GFP did not arrest. Bars, 10 μm.

ies against Cdc27, a component of the APC, prevents cyclin A degradation in vivo, and both APC^{Cdc20} and APC^{Cdh1} will ubiquitylate cyclin A in vitro. Currently, it is thought that the APC needs to bind Cdc20 to be active in mitosis (for review see Morgan, 1999) and that Cdc20 is required for cyclin A degradation in *Drosophila* and *Xenopus* extracts because mutations in the Cdc20 homologue, *fizzy*, or anti-Fizzy antibodies, stabilize cyclin A (Dawson et al., 1995; Sigrist et al., 1995; Lorca et al., 1998). Furthermore, Geley et al. *(*2001) in this issue have found that anti-Cdc20 antibodies prevent cyclin A degradation in human cells. However, in animal cells, evidence indicates that during prometaphase the spindle checkpoint keeps Cdc20 inactive until all the chromosomes have attached to both poles of the spindle (Li et al., 1997; Fang et al., 1998; Gorbsky et al., 1998; Dobles et al., 2000). Yet here we show that cyclin A is degraded both in prometaphase and in the presence of taxol, indicating that if APC^{Cdc20} does degrade cyclin A, it is not inhibited by the spindle checkpoint. Moreover, eliminating the spindle checkpoint by introducing dominant negative Bub1 causes cyclin B1 to begin to be degraded at the same time as cyclin A (Geley et al., 2001, this issue). Perhaps there are different forms of APC^{Cdc20}, some of which are not inhibited by the spindle checkpoint and can recognize cyclin A, but not cyclin B1. In this respect, it may be relevant that Cdc20 has been reported to bind directly to the NH_2 terminus of cyclin A (Ohtoshi et al., 2000). Alternatively, Geley et al. (2001) suggest that cyclin A may simply be a much better substrate for APC^{Cdc20}, such that it can still be degraded when the spindle checkpoint reduces the availability of active Cdc20.

Cyclin A Degradation Is D-Box Independent, but Requires Cdk Binding for Its Correct Timing

The conservation through evolution of the relative timing of cyclin A and B proteolysis indicates that delaying cyclin A degradation until metaphase might have an adverse effect on mitosis. Indeed, Clb5, the budding yeast cyclin most analogous in function to cyclin A, must be destroyed to allow Clb2 to be degraded, possibly because Clb5 phosphorylates Cdh1 and keeps it inactive (Shirayama et al., 1999). To determine whether the prometaphase destruction of cyclin A is essential for normal mitosis, we attempted to alter its timing by mutating the cyclin A D-box. To our surprise, the D-box is not required for cyclin A degradation in human cells, in contrast to the D-box–dependent proteolysis of *Xenopus* cyclin A1 in *Xenopus* egg extract (Kobayashi et al., 1992). Possibly the mitotic degradation of human somatic cyclin A differs from that of the embryonic *Xenopus* cyclin A1 in meiosis and early embryos. Alternatively, these contradictions may be due to a difference between in vivo and in vitro systems.

We also find that cyclin A degradation does not require Cdk binding, again in contrast to the behavior of cyclin A in *Xenopus* egg extracts (Stewart et al., 1994; Geley et al.,

2001, this issue). However, an inability to bind its Cdk does alter the timing of cyclin A degradation, delaying this until anaphase. Cyclin A and Cdk2 may be recognized as a complex by the prometaphase ubiquitination and/or degradation machinery, or Cdk2 might induce conformational changes in cyclin A required for its prometaphase destruction. The degradation of non-Cdk–binding cyclin A–GFP in anaphase is D-box independent, indicating that it is distinct from that of cyclin B1 and securin in metaphase (Clute and Pines, 1999; Hagting, A., N. den Elzen, and J. Pines, manuscript in preparation).

Proteolysis Is Required for Chromosome Alignment and Anaphase

Increasing the level of cyclin A in mitosis causes a delay in chromosome alignment and the start of anaphase. During this delay, the chromosomes are dynamic: individual chromosomes move independently to and from the cell equator. In the delay caused by cyclin A, it is obvious that sister chromatids have not segregated because misaligned chromosomes return to the metaphase plate in both PtK_1 and HeLa cells. Eventually, cells segregate their chromosomes synchronously in an apparently normal anaphase.

Our observations that the length of the delay is directly related to the amount of cyclin A–GFP, and that before chromosomes align the amount of cyclin A–GFP has to be reduced below a threshold equivalent to 0.2 times the amount of cyclin A in a G2 phase cell, indicate that the level of cyclin A specifically affects chromosome alignment and anaphase. Moreover, chromosome alignment can be prevented by inhibiting the 26S proteasome from prophase onwards, providing further evidence that a protein or proteins must be degraded during prophase and/or prometaphase for chromosome alignment and anaphase. Consistent with this, a dominant negative form of UBC3 blocks chromosome congression in PtK_1 cells (Bastians et al., 1999), although this protein usually acts in conjunction with the Skp1-Cullin-F-box (SCF) complex, not the APC.

We are currently investigating the mechanism by which cyclin A delays chromosome alignment and anaphase. The lag does not appear to result from cyclin A–associated Cdk activity per se, because expressing the nondegradable ΔN97 cyclin A–GFP construct does not arrest cells before chromosome alignment (Fig. 6; Geley et al., 2001, in this issue). Instead, these cells proceed normally until they arrest in anaphase B or telophase. This is in contrast to the metaphase delay reported for the overexpression of nondegradable cyclin A in *Drosophila* (Sigrist et al., 1995). However, in this study, anaphase and telophase cells could also be observed, leading the authors to conclude that the metaphase arrest is leaky. An alternative explanation congruent with our results is that cells arrest in anaphase with chromosomes that are highly dynamic and often appear at the cell equator (Fig. 6 A). Moreover, Su and Jaklevic (2001) have shown recently that *Drosophila* cells at the gastrula stage delay in metaphase after DNA damage, and this delay correlates with the stabilization of cyclin A. Furthermore, mutant cells lacking cyclin A are unable to delay in mitosis and enter anaphase with an increased number of lagging chromosomes (Su and Jaklevic, 2001). Thus, there are conditions when the ability of cyclin A to prevent anaphase may be used as part of a checkpoint to safeguard genomic integrity. In agreement with our results, Su and Jaklevic (2001) also found that the length of the metaphase delay depended on the gene dosage of cyclin A.

We favor the interpretation that the ability of cyclin A–GFP to delay chromosome alignment and anaphase depends on its ability to be degraded. Cyclin A–GFP might compete for a limiting component of the degradation machinery and prevent the degradation of another protein(s) whose removal is required for chromosome alignment and anaphase. However, we cannot discount the alternative possibility that the inability of ΔN97 cyclin A–GFP to delay chromosome alignment and anaphase is due to its inability to phosphorylate key substrates of cyclin A/CDK involved in chromosome alignment and anaphase. The observation that *Drosophila* cells lacking cyclin A cannot delay in metaphase in response to DNA damage (Su and Jaklevic, 2001) may also indicate that cyclin A directly inhibits anaphase.

We think it is unlikely that increasing cyclin A levels delays mitosis by activating the spindle checkpoint, because none of the misaligned chromosomes in cyclin A–GFP-delayed cells stained for Mad2. This is prima facie evidence that the spindle checkpoint is not active and that all the chromosomes should be attached to both poles of the spindle (Chen et al., 1996; Li and Benezra, 1996; Waters et al., 1998). Furthermore, cyclin B1–YFP, whose degradation is prevented by the spindle checkpoint (Clute and Pines, 1999), is degraded during a cyclin A–induced mitotic delay. Lastly, abrogating the spindle checkpoint altogether using a dominant negative Bub1 construct does not eliminate the cyclin A–induced delay. Thus, it is more likely that increasing cyclin A levels induce a delay through proteins that are involved in chromosome alignment and the initiation of anaphase, but not the spindle checkpoint, such as motor proteins implicated in chromosome congression.

Intringuingly, we find that adding taxol to cells that are degrading cyclin B1 in the presence of excess cyclin A does not immediately stop cyclin B1 proteolysis. Instead, it appears that cyclin A has to fall below a threshold level before cyclin B1 becomes stable. Thus, rather than activating the spindle checkpoint, cyclin A may perturb the spindle checkpoint signal. In support of this, we have observed that cells expressing high amounts of cyclin A sometimes begin to degrade cyclin B1 just after NEBD, in a similar manner to cells expressing dominant negative Bub1. If excess cyclin A does interfere with the spindle checkpoint, then this may have the same root cause as the inability to align chromosomes, i.e., cyclin A may affect the structure and or function of the kinetochore.

Is Sister Chromatid Segregation Dependent on Chromosome Alignment?

It is important to determine the relationship between the delay in chromosome alignment and the delay in anaphase caused by cyclin A. Preventing chromosome alignment might directly cause the delay in the initiation of anaphase. Alternatively, cyclin A may prevent chromosome alignment and anaphase through separate pathways. In this respect, our preliminary observations indicate that the destruction of cyclin B1–YFP and hSecurin-YFP, an in vivo marker for securin (Hagting, A., N. den Elzen, and J. Pines, manuscript in preparation), may be slower in cyclin A–CFP expressing cells, and Geley et al. (page 137) in this issue also find that overexpressing cyclin A can affect

the destruction of cyclin B1. Whatever the mechanism, it has important implications for how anaphase is regulated. Finally, our studies show that the cleavage furrow is correctly set up at the equator of the cell without the need for a stable metaphase plate. Further studies will be needed to determine the relationship between proteolysis, chromosome alignment, and the initiation of anaphase and cytokinesis in animal cells.

We are grateful to Carl Mann (CEA, Saclay, France) for CAK cDNA, George Banting (University of Bristol, Bristol, UK) for GroEL/GroES chaperonin cDNA, Stephan Geley and Tim Hunt (Imperial Cancer Research Fund) for dominant negative Bub1, and to Michel Bornens (Institut Curie, Paris, France) for anti-CTR453 serum. We thank Anja Hagting for pCMX-cyclin B1-YFP cDNA, Mark Jackman for Cyclin A–GFP/Cdk2 and Cdk2 proteins, Paul Clute for cyclin A–GFP protein, Nobu Furuno for Cyclin A/Cdk2, and Tim Bradbeer for GST-CAK protein. Many thanks to all members of the laboratory, especially Anja Hagting and Mark Jackman, for helpful advice and discussions, and to Stephan Geley and Tim Hunt for discussions and communicating unpublished results. We would also like to thank the reviewer who suggested performing the experiments in Fig. 5, C and D.

N. den Elzen is supported by an Association of Commonwealth Universities scholarship and this work was supported by a Cancer Research Campaign program grant to J. Pines.

Submitted: 17 October 2000
Revised: 22 January 2001
Accepted: 24 January 2001

References

Alexandru, G., W. Zachariae, A. Schleiffer, and K. Nasmyth. 1999. Sister chromatid separation and chromosome re-duplication are regulated by different mechanisms in response to spindle damage. *EMBO (Eur. Mol. Biol. Organ.) J.* 18:2707–2721.

Bailly, E., J. Pines, T. Hunter, and M. Bornens. 1992. Cytoplasmic accumulation of cyclin B1 in human cells: association with a detergent-resistant compartment and with the centrosome. *J. Cell Sci.* 101:529–545.

Bastians, H., L.M. Topper, G.L. Gorbsky, and J.V. Ruderman. 1999. Cell cycle-regulated proteolysis of mitotic target proteins. *Mol. Biol. Cell.* 10:3927–3941.

Chen, R.H., J.C. Waters, E.D. Salmon, and A.W. Murray. 1996. Association of spindle assembly checkpoint component XMAD2 with unattached kinetochores. *Science*. 274:242–246.

Clute, P., and J. Pines. 1999. Temporal and spatial control of cyclin B1 destruction in metaphase. *Nat. Cell Biol.* 1:82–87.

Dawson, I.A., S. Roth, and S. Artavanis-Tsakonas. 1995. The *Drosophila* cell cycle gene *fizzy* is required for normal degradation of cyclins A and B during mitosis and has homology to the CDC20 gene of *Saccharomyces cerevisiae*. *J. Cell Biol.* 129:725–737.

Dobles, M., V. Liberal, M.L. Scott, R. Benezra, and P.K. Sorger. 2000. Chromosome missegregation and apoptosis in mice lacking the mitotic checkpoint protein Mad2. *Cell*. 101:635–645.

Fang, G., H. Yu, and M.W. Kirschner. 1998. The checkpoint protein MAD2 and the mitotic regulator CDC20 form a ternary complex with the anaphase-promoting complex to control anaphase initiation. *Genes Dev*. 12:1871–1883.

Félix, M.-A., J.-C. Labbé, M. Dorée, T. Hunt, and E. Karsenti. 1990. Triggering of cyclin degradation in interphase extracts of amphibian eggs by cdc2 kinase. *Nature*. 346:379–382.

Furuno, N., N. den Elzen, and J. Pines. 1999. Human cyclin A is required for mitosis until mid prophase. *J. Cell Biol.* 147:295–306.

Geley, S., E. Kramer, C. Gieffers, J. Gannon, J.-M. Peters, and T. Hunt. 2001. Anaphase-promoting complex/cyclosome–dependent proteolysis of human cyclin A starts at the beginning of mitosis and is not subject to the spindle assembly checkpoint. *J. Cell Biol.* 153:137–147.

Girard, F., A. Fernandez, and N. Lamb. 1995. Delayed cyclin A and B1 degradation in non-transformed mammalian cells. *J. Cell Sci*. 108:2599–2608.

Glotzer, M., A.W. Murray, and M.W. Kirschner. 1991. Cyclin is degraded by the ubiquitin pathway. *Nature*. 349:132–138.

Gorbsky, G.J., R.H. Chen, and A.W. Murray. 1998. Microinjection of antibody to Mad2 protein into mammalian cells in mitosis induces premature anaphase. *J. Cell Biol.* 141:1193–1205.

Hagting, A., M. Jackman, K. Simpson, and J. Pines. 1999. Translocation of cyclin B1 to the nucleus at prophase requires a phosphorylation-dependent nuclear import signal. *Curr. Biol*. 9:680–689.

Hardwick, K.G. 1998. The spindle checkpoint. *Trends Genet*. 14:1–4.

Hershko, A., and A. Ciechanover. 1998. The ubiquitin system. *Annu. Rev. Biochem*. 67:425–479.

Hershko, A., D. Ganoth, V. Sudakin, A. Dahan, L.H. Cohen, F.C. Luca, J.V. Ruderman, and E. Eytan. 1994. Components of a system that ligates cyclin to ubiquitin and their regulation by the protein kinase cdc2. *J. Biol. Chem*. 269:4940–4946.

Holloway, S.L., M. Glotzer, R.W. King, and A.W. Murray. 1993. Anaphase is initiated by proteolysis rather than by the inactivation of maturation-promoting factor. *Cell*. 73:1393–1402.

Howell, B.J., D.B. Hoffman, G. Fang, A.W. Murray, and E.D. Salmon. 2000. Visualization of Mad2 dynamics at kinetochores, along spindle fibers, and at spindle poles in living cells. *J. Cell Biol*. 150:1233–1250.

Hunt, T., F.C. Luca, and J.V. Ruderman. 1992. The requirements for protein synthesis and degradation, and the control of destruction of cyclins A and B in the meiotic and mitotic cell cycles of the clam embryo. *J. Cell Biol*. 116: 707–724.

King, R.W., J.-M. Peters, S. Tugendreich, M. Rolfe, P. Hieter, and M.W. Kirschner. 1995. A 20S complex containing CDC27 and CDC16 catalyzes the mitosis-specific conjugation of ubiquitin to cyclin B. *Cell*. 81:279–288.

King, R.W., R.J. Deshaies, J.M. Peters, and M.W. Kirschner. 1996a. How proteolysis drives the cell cycle. *Science*. 274:1652–1659.

King, R.W., M. Glotzer, and M.W. Kirschner. 1996b. Mutagenic analysis of the destruction signal of mitotic cyclins and structural characterization of ubiquitinated intermediates. *Mol. Biol. Cell*. 7:1343–1357.

Klotzbucher, A., E. Stewart, D. Harrison, and T. Hunt. 1996. The "destruction box" of cyclin A allows B-type cyclins to be ubiquitinated, but not efficiently destroyed. *EMBO (Eur. Mol. Biol. Organ.) J*. 15:3053–3064.

Kobayashi, H., E. Stewart, R. Poon, J.P. Adamczewski, J. Gannon, and T. Hunt. 1992. Identification of the domains in cyclin A required for binding to, and activation of, p34cdc2 and p32cdk2 protein kinase subunits. *Mol. Biol. Cell*. 3:1279–1294.

Krude, T., M.R. Jackman, J.N. Pines, and R.A. Laskey. 1997. Cyclin/Cdk-dependent initiation of DNA replication in a human cell-free system. *Cell*. 87:109–119.

Lehner, C.F., and P.H. O'Farrell. 1990. The roles of *Drosophila* cyclins A and B in mitotic control. *Cell*. 61:535–547.

Li, X., and R.B. Nicklas. 1995. Mitotic forces control a cell-cycle checkpoint. *Nature*. 373:630–632.

Li, Y., and R. Benezra. 1996. Identification of a human mitotic checkpoint gene: hsMAD2. *Science*. 274:246–248.

Li, Y., C. Gorbea, D. Mahaffey, M. Rechsteiner, and R. Benezra. 1997. MAD2 associates with the cyclosome/anaphase-promoting complex and inhibits its activity. *Proc. Natl. Acad. Sci. USA*. 94:12431–12436.

Lorca, T., A. Castro, A.M. Martinez, S. Vigneron, N. Morin, S. Sigrist, C. Lehner, M. Doree, and J.C. Labbe. 1998. Fizzy is required for activation of the APC/cyclosome in *Xenopus* egg extracts. *EMBO (Eur. Mol. Biol. Organ.) J*. 17:3565–3575.

Lorca, T., A. Devault, P. Colas, L.A. Van, D. Fesquet, J.B. Lazaro, and M. Doree. 1992a. Cyclin A-Cys41 does not undergo cell cycle-dependent degradation in *Xenopus* extracts. *FEBS Lett*. 306:90–93.

Lorca, T., J.C. Labbe, A. Devault, D. Fesquet, U. Strausfeld, J. Nilsson, P.A. Nygren, M. Uhlen, J.C. Cavadore, and M. Doree. 1992b. Cyclin A-cdc2 kinase does not trigger but delays cyclin degradation in interphase extracts of amphibian eggs. *J. Cell Sci*. 102:55–62.

Luca, F.C., and J.V. Ruderman. 1989. Control of programmed cyclin destruction in a cell-free system. *J. Cell Biol.* 109:1895–1909.

Luca, F.C., E.K. Shibuya, C.E. Dohrmann, and J.V. Ruderman. 1991. Both cyclin A delta 60 and B delta 97 are stable and arrest cells in M-phase, but only cyclin B delta 97 turns on cyclin destruction. *EMBO (Eur. Mol. Biol. Organ.) J*. 10:4311–4320.

Minshull, J., R. Golsteyn, C.S. Hill, and T. Hunt. 1990. The A- and B-type cyclin associated cdc2 kinases in *Xenopus* turn on and off at different times in the cell cycle. *EMBO (Eur. Mol. Biol. Organ.) J*. 9:2865–2875.

Morgan, D.O. 1999. Regulation of the APC and the exit from mitosis. *Nat. Cell Biol*. 1:E47–E53.

Norbury, C., and P. Nurse. 1993. Animal cell cycles and their control. *Annu. Rev. Biochem.* 61:441–470.

Ohtoshi, A., T. Maeda, H. Higashi, S. Ashizawa, and M. Hatakeyama. 2000. Human p55(CDC)/Cdc20 associates with cyclin A and is phosphorylated by the cyclin A-Cdk2 complex. *Biochem. Biophys. Res. Commun*. 268:530–534.

Ookata, K., S. Hisanaga, T. Okano, K. Tachibana, and T. Kishimoto. 1992. Relocation and distinct subcellular localization of p34cdc2-cyclin B complex at meiosis reinitiation in starfish oocytes. *EMBO (Eur. Mol. Biol. Organ.) J*. 11:1763–1772.

Pagano, M., R. Pepperkok, F. Verde, W. Ansorge, and G. Draetta. 1992. Cyclin A is required at two points in the human cell cycle. *EMBO (Eur. Mol. Biol. Organ.) J*. 11:961–971.

Pines, J. 1997. Localization of cell cycle regulators by immunofluorescence. *Methods Enzymol.* 283:99–113.

Pines, J., and T. Hunter. 1990. Human cyclin A is adenovirus E1A-associated protein p60, and behaves differently from cyclin B. *Nature*. 346:760–763.

Pines, J., and T. Hunter. 1991. Human cyclins A and B are differentially located in the cell and undergo cell cycle–dependent nuclear transport. *J. Cell Biol.* 115:1–17.

Rieder, C.L., A. Schultz, R. Cole, and G. Sluder. 1994. Anaphase onset in ver-

tebrate somatic cells is controlled by a checkpoint that monitors sister kinetochore attachment to the spindle. *J. Cell Biol.* 127:1301–1310.

Rieder, C.L., R.W. Cole, A. Khodjakov, and G. Sluder. 1995. The checkpoint delaying anaphase in response to chromosome monoorientation is mediated by an inhibitory signal produced by unattached kinetochores. *J. Cell Biol*. 130:941–948.

Shirayama, M., A. Toth, M. Galova, and K. Nasmyth. 1999. APC(Cdc20) promotes exit from mitosis by destroying the anaphase inhibitor Pds1 and cyclin Clb5. *Nature*. 402:203–207.

Sigrist, S., H. Jacobs, R. Stratmann, and C.F. Lehner. 1995. Exit from mitosis is regulated by *Drosophila* fizzy and the sequential destruction of cyclins A, B and B3. *EMBO (Eur. Mol. Biol. Organ.) J*. 14:4827–4838.

Stewart, E., H. Kobayashi, D. Harrison, and T. Hunt. 1994. Destruction of *Xenopus* cyclins A and B2, but not B1, requires binding to p34cdc2. *EMBO (Eur. Mol. Biol. Organ.) J*. 13:584–594.

Su, T.T., and B. Jaklevic. 2001. DNA damage leads to a cyclin A-dependent delay in metaphase-anaphase transition in the *Drosophila* gastrula. *Curr. Biol*. 11:8–17.

Sudakin, V., D. Ganoth, A. Dahan, H. Heller, J. Hershko, F.C. Luca, J.V. Ruderman, and A. Hershko. 1995. The cyclosome, a large complex containing cyclin-selective ubiquitin ligase activity, targets cyclins for destruction at the end of mitosis. *Mol. Biol. Cell*. 6:185–197.

Taylor, S.S. 1999. Chromosome segregation: dual control ensures fidelity. *Curr. Biol*. 9:R562–R564.

Taylor, S.S., and F. McKeon. 1997. Kinetochore localization of murine Bub1 is required for normal mitotic timing and checkpoint response to spindle damage. *Cell*. 89:727–735.

Tobey, R.A., N. Oishi, and H.A. Crissman. 1990. Cell cycle synchronization: reversible induction of G2 synchrony in cultured rodent and human diploid fibroblasts. *Proc. Natl. Acad. Sci. USA*. 87:5104–5108.

Townsley, F.M., A. Aristarkhov, S. Beck, A. Hershko, and J.V. Ruderman. 1997. Dominant-negative cyclin-selective ubiquitin carrier protein E2-C/UbcH10 blocks cells in metaphase. *Proc. Natl. Acad. Sci. USA*. 94:2362–2367.

Waters, J.C., R.H. Chen, A.W. Murray, and E.D. Salmon. 1998. Localization of Mad2 to kinetochores depends on microtubule attachment, not tension. *J. Cell Biol*. 141:1181–1191.

Wheatley, S.P., E.H. Hinchcliffe, M. Glotzer, A.A. Hyman, G. Sluder, and Y. Wang. 1997. CDK1 inactivation regulates anaphase spindle dynamics and cytokinesis in vivo. *J. Cell Biol*. 138:385–393.

Whitfield, W.G.F., C. Gonzalez, G. Maldonado-Codina, and D.M. Glover. 1990. The A- and B-type cyclins of *Drosophila* are accumulated and destroyed in temporally distinct events that define separable phases of the G2-M transition. *EMBO (Eur. Mol. Biol. Organ.) J*. 9:2563–2572.

Yamamoto, A., V. Guacci, and D. Koshland. 1996. Pds1p, an inhibitor of anaphase in budding yeast, plays a critical role in the APC and checkpoint pathway(s). *J. Cell Biol*. 133:99–110.

Yamano, H., C. Tsurumi, J. Gannon, and T. Hunt. 1998. The role of the destruction box and its neighbouring lysine residues in cyclin B for anaphase ubiquitin-dependent proteolysis in fission yeast: defining the D-box receptor. *EMBO (Eur. Mol. Biol. Organ.) J*. 17:5670–5678.